Supporting Information

Unveiling the spatial rearrangements of exhausted immobilised multi-enzyme systems through cryo-X-ray fluorescence nanoprobe imaging

Javier Santiago-Arcos,[a] Murielle Salome,[b] Fernando López-Gallego*[a,c] and Carlos Sanchez-Cano*[c,d,e]

[a] Center for Cooperative Research in Biomaterials (CIC biomaGUNE) - Basque Research and Technology Alliance (BRTA) Paseo de Miramón, 182, 20014 Donostia-San Sebastián, Spain

[b] ESRF, The European Synchrotron, 71 Avenue des Martyrs, CS40220, 38043 Grenoble Cedex 9, France

[c] Ikerbasque, Basque Foundation for Science, Plaza Euskadi 5, 48009 Bilbao, Spain

[d] Donostia International Physics Center, Paseo Manuel de Lardizabal 4, Donostia, 20018, Spain

[e] Polimero eta Material Aurreratuak: Fisika, Kimika eta Teknologia, Kimika Fakultatea, Euskal Herriko Unibertsitatea UPV/EHU, 20018 Donostia-San Sebastian, Spain

E-mail: flopez@cicbiomagune.es; carlos.sanchez@dipc.org

Materials and Methods

Materials.

The enzymes alcohol dehydrogenase (ADH), containing a His-Tag, from *Bacillus stearothermophilus* (BsADH) was produced as previously reported,[1] whereas the lacasse from *Aspergillus.sp* (AsLAC) was purchased from Merck group (Novozym 51003). Four percent cross-linked agarose (AG) beads (particle size 50−150 μm; pore diameter 300 nm) were purchased from Agarose Bead Technologies (Madrid, Spain). Compounds such as ethylenediamine (EDA), imidazole, iminodiacetic acid, cobalt chloride, sodium periodate, sodium hydroxide fluorescein isothiocyanate (FITC), rhodamine B isothiocyanate, sodium acetate, sodium chloride, sodium phosphate, sodium bicarbonate, 1,5-pentanediolwere acquired from Merck group. All other reagents were of analytical grade.

Preparation of agarose microbeads functionalised with cobalt-chelates and primary amino groups (AG-A/Co^{2+}).

The preparation of the bifunctional carrier was carried out following protocols previously reported in our group.[2] For the first step, we prepared activated agarose with epoxy groups (AG-E) as described elsewhere.[3] Then, we functionalised the AG-E with iminodiacetic acid (AG-E/IDA) by preparing a suspension of 10 g (≈14 mL) of AG-E in 100 mL of 0.5 M iminodiacetic acid at pH 11. The suspension was maintained under gentle agitation at 200 rpm for 1 h at room temperature (RT). Afterwards, the beads were collected by filtration and rinsed with 10 volumes of water. Once AG-E/IDA was obtained, we introduced amino groups by incubating it overnight with 10 volumes of 2 M ethylenediamine at pH 11 (AG-A/IDA) under gentle agitation at 200 rpm at room temperature. Then, agarose microbeads were filtered and gently rinsed with water. Finally, to introduce the metal group, the support was incubated with 10 volumes of 30 mg mL^{-1} of $CoCl_2$ for 2 h at room temperature (AG-A/Co^{2+}). In the end, the support was filtered and washed with abundant water and stored at 4 °C.

Enzyme co-immobilization.

Enzyme co-immobilisation was conducted incorporating the enzymes sequentially to the AG-A/Co^{2+} beads. 10 mL of AsLAC in 5 mM sodium acetate buffer at pH 5 was first incubated with 1 g of AG-A/Co^{2+} for 2 h at 40 rpm and 4 °C. Afterwards, the suspension was filtered and 10 mL of a solution of BsADH in 5 mM sodium phosphate buffer at pH 7 was added, followed by incubation for 15 min at 4 °C and 40 rpm. Finally, the biocatalyst was filtered off and washed with 5 mM sodium phosphate buffer pH 7 and stored at 4 °C.

Enzyme Activity Assays.

Enzyme activities were spectrophotometrically measured in transparent 96-well microplates with a flat bottom (Nunc), employing a Microplate Reader Epoch 2 (BioTek Instruments) provided with the software Gen5.

ADH Activity.

Two hundred microliters of a reaction mixture containing 10 mM of 1,5-pentanediol and 1 mM of NAD^+ in sodium phosphate buffer at pH 8 were incubated with 5 μL of enzymatic solution or 10 μL of suspension (properly diluted) at 30 °C. The increase in the absorbance at 340 nm due to the reduction of NAD^+ was recorded. One unit of activity was defined as the amount of enzyme that was required to reduce 1 μmol of NAD^+ to NADH per minute at the assayed conditions.

Lacasse Activity.
Two hundred microliters of a reaction mixture containing 50 μM of ABTS in 5 mM sodium acetate buffer pH 5 at 30°C were incubated with 5 μL of enzymatic solution or 10 μL of suspension (properly diluted) at 30 °C. The oxidation of NADH was monitored as a decrease in the absorbance at 420 nm. One unit of activity was defined as the amount of enzyme that was required to oxidise 1 μmol of ABTS per minute at the assayed conditions.

Thermal Inactivation.
Thermal inactivation kinetics of the biocatalyst was conducted by incubating a solution or a suspension of immobilised enzymes in 5 mM sodium phosphate buffer pH 7 at 70°C for 2 hours due to previous T_{50} elucidated in previous work for BsADH.[4]

Protein Labelling with Fluorescent Probes.
Fluorescent labelling was done accordingly with a methodology reported elsewhere.[5] An enzyme solution (typically 0.25 mg mL^{-1}) in 100 mM of sodium bicarbonate buffer at pH 8.5 was mixed (1:10 molar ratio) with either rhodamine B isothiocyanate (RhoB) for BsADH or fluorescein isothiocyanate (FITC) for AsLAC in dimethyl sulfoxide (DMSO) (5 mg·mL^{-1}) and incubated 1 h with gentle agitation at 25 °C in darkness. Afterward, the remaining fluorophore was eliminated by dialysis through a centrifugal filter unit (cut off of 10 kDa) with 25 mM sodium phosphate buffer pH 8.0.

Batch Reactions and Recycling of co-immobilised Enzymes.
Heterogeneous biocatalysts (50 mg) were placed inside a capped plastic tube (2 mL) containing 500 μL of a reaction mixture consisting of 20 mM of 1,5-pentanediol, 1 mM of NAD^+, 1 mM of acetoseryngone in 5 mM sodium phosphate buffer pH 7 allowing atmospheric oxygen supplementation by punching the tap with an open needle. Reactions were incubated at 30 °C at 250 rpm inside an orbital incubator during 24 hours per cycle.

Chromatographic Methods. Gas Chromatography (GC).
Prior to GC analysis, 50 μL of the reaction sample was mixed with 200 μL of ethyl acetate to perform a liquid−liquid extraction of the compounds of interest containing 2 mM eicosane as the external standard. After the extraction, 30−50 mg of anhydrous $MgSO_4$ was added to dry samples before GC analysis. Gas chromatography analyses were carried out in an Agilent 8890 GC system chromato- graph using a J&W HP-5 GC column (30 m × 0.32 mm × 0.25 μm), helium as the support gas, and equipped with a flame ionisation detector (FID). The injector was set at 280°C and the FID at 300°C. Separation of extracted compounds in ethyl acetate was done by the following temperature program: the initial temperature at 60 °C, maintained 2 min, ramp to 160 °C at a rate of 10 °C min^{-1}, ramp 2− 240 °C at a rate of 20 °C min^{-1} and finally maintained 4 min. A calibration curve was carried out for the tetrahydro-2H-pyran-2- ol to elucidate the final concentration of it, whereas the 1,5-pentanediol consumption was determined through dividing the area of the sample after 24 hour reaction by the initial sample area. All values were normalised by eicosane as an internal standard in all samples. Retention times for 1,5-pentanediol, 5.6 min, tetrahydro-2H-pyran-2- ol, 3.4 min, δ-valerolactone, 5.8 min, and eicosane (external standard), 16.4 min.

Confocal Laser Scanning Microscopy (CLSM) Imaging.
The distribution of immobilised fluorophore-labelled proteins was analysed with a confocal microscope Espectral ZEISS LSM 510 with an excitation laser for FITC of λ_{ex}:

488 nm and for Rhodamine-B λ_{ex}: 561 nm. Confocal imaging was carried out at both 20× (water, 1.2 NA) objectives and a 1:200 (w/v) buffered suspension in 25 mM phosphate at pH 7. The resulting micrographs were analysed with Fiji open source processing package[6] using an image analytical routine previously reported.[7] From confocal images, we obtained an average and normalised fluorescence radius profile, using FIJI software and its plugin module for radial profile generation (developed by Paul Baggethun). Subsequently, a Gaussian fit was applied to the obtained profiles of at least 10 single beads. Subsequently, we searched for the fitted data point that corresponds to 50% of the maximum normalised fluorescence fitted peak (yFWHM), and the corresponding radius coordinate (xFWHM) to that data point was then subtracted from the radius (R) of the analysed bead to finally obtain the full width at half-maximum (FWHM), which means the infiltration distance of the enzyme into the bead surface. Dividing this infiltration distance between the radius size, we obtained the relative infiltration distance.

XRF

AG-A/Co^{2+} microbeads were immobilised on Silicon nitride TEM windows (frame size = 5x5 mm, frame thickness = 200 μm, membrane size 1.5x1.5 mm, membrane thickness 500 nm; Silson Ltd, UK) prepared by using glow discharge. Then, the membranes were immersed in water, blotted (2s) with filter paper and manually plunge-freezed in liquid ethane. The frozen membranes were transferred to holders that were 3D-printed inhouse for storage and transport, and kept under cryogenic conditions in liquid nitrogen until measurements were performed. All synchrotron experiments were performed at the beamline ID16A at the European Synchrotron Radiation Facility (ESRF, Grenoble, France). XRF maps of individual cells were acquired under cryogenic conditions using two six element silicon drift diode detectors with an area of 3 cm^2 at a distance of 3 cm from the sample. The incident beam energy was fixed to 17 keV (with a photon flux of 1.55 $x10^{11}$ ph/s) and focused to 48.6 x 41.6 nm^2 (horizontal x vertical; FWHM). Coarse scans to detect areas of interest were done using 400x400 nm^2 steps (50 ms dwell time), and fine mapping of the beads was performed using a step size of 100x100 nm^2 (50 ms dwell time). Summed emission spectra were fitted to generate elemental maps using PyMCA toolkit (ESRF),[8] that were analysed using Fiji open source processing package.[6]

Additional Figures

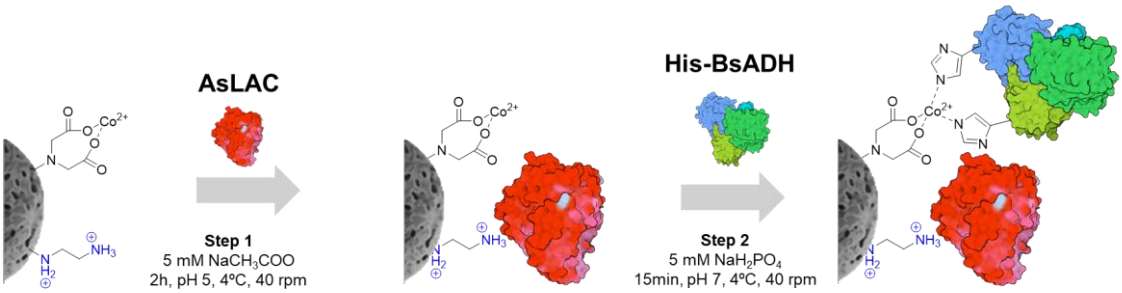

Figure S1. Immobilisation sequence of AsLAC and BsADH on AG-A/Co^{2+} support. AsLAC was first incubated under the described conditions (step 1). Then, the supernatant was removed, and the support was incubated with the solution of BsADH under the described conditions (step 2). Finally, the bi-enzyme heterogeneous biocatalyst was washed with 10 mM sodium phosphate at pH 7 and stored for further use.

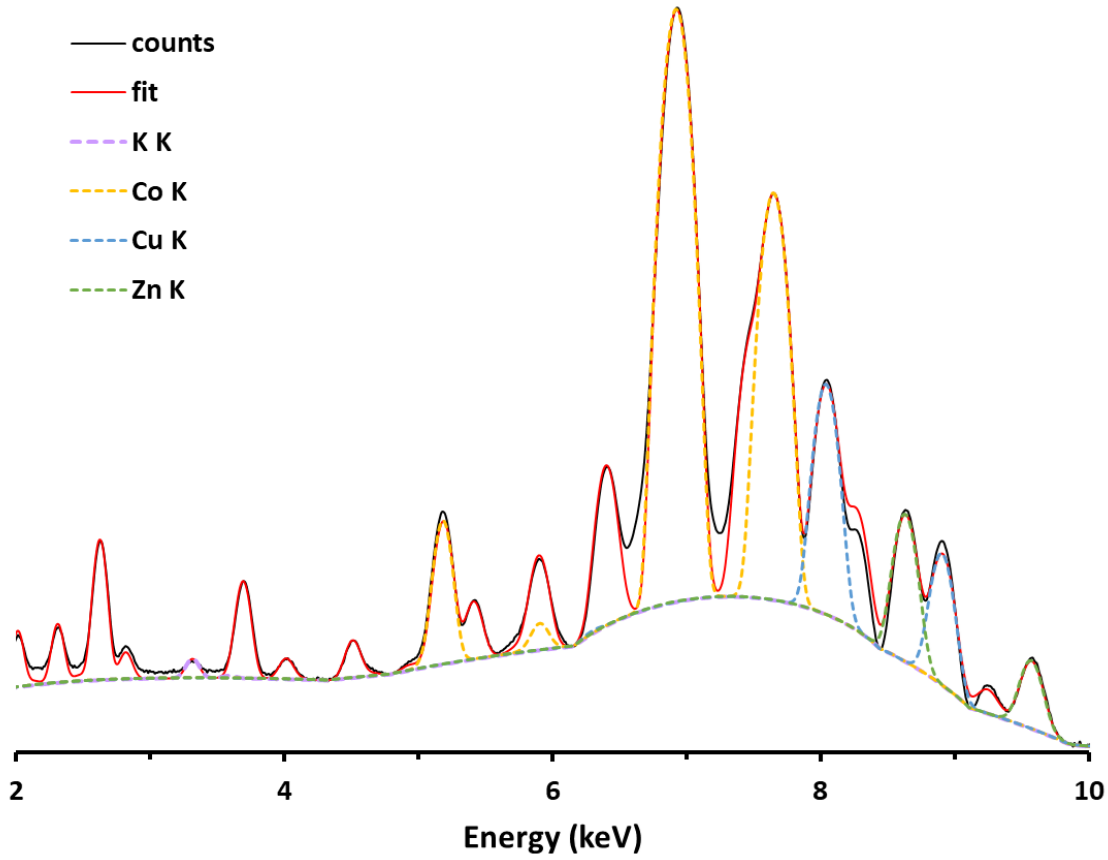

Figure S2. Representative XRF spectrum of AG-A/Co^{2+} beads bearing BsADH and AsLAC. Data was fitted using PyMCa toolkit (ESRF).[8] The contribution from K K (purple), Co K (yellow), Cu K (blue) and Zn K (green) emission lines are shown.

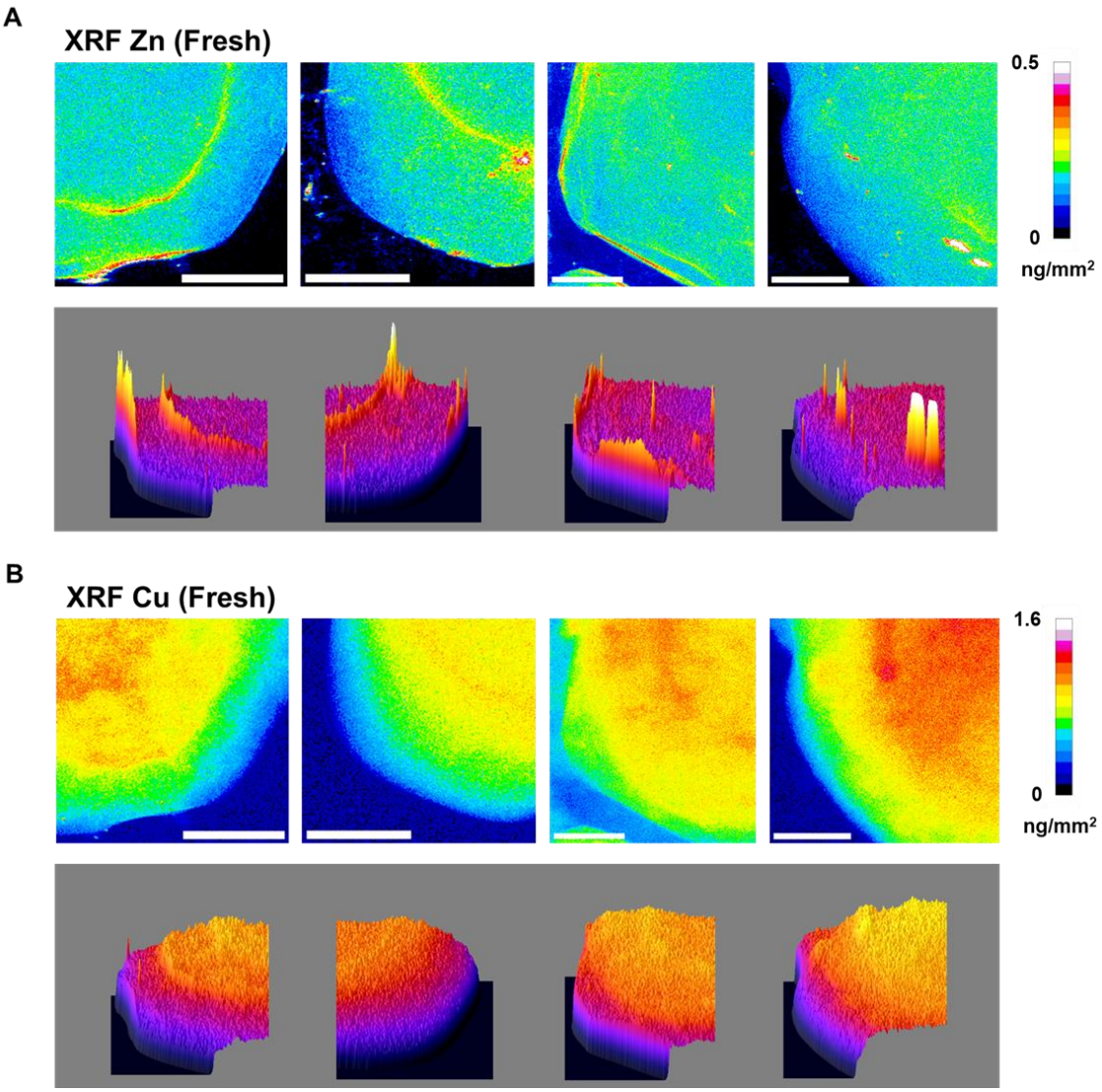

Figure S3. Quantitative XRF maps (top) and 3D intensity profile plots (bottom) of Zn (A) and Cu (B) of several AG-A/Co^{2+} beads bearing BsADH and AsLAC. Pixel intensity in XRF maps represents metal density according to colour scale. Scale bar 10 µm.

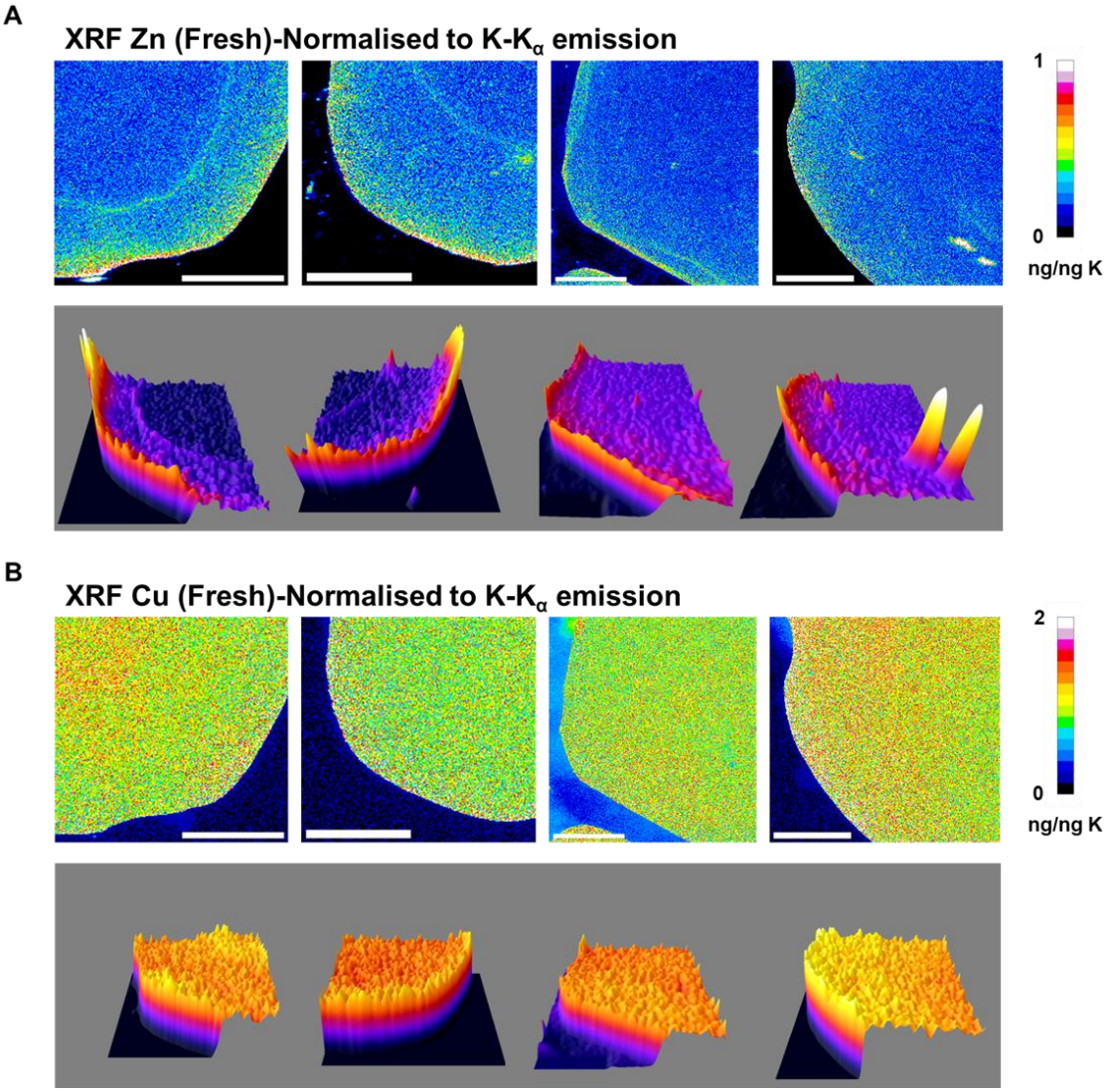

Figure S4. Quantitative XRF maps (top) and 3D intensity profile plots (bottom) of Zn (A) and Cu (B) normalised to K content/pixel of several AG-A/Co^{2+} beads bearing BsADH and AsLAC. Pixel intensity in XRF maps represents metal density according to colour scale. Scale bar 10 µm.

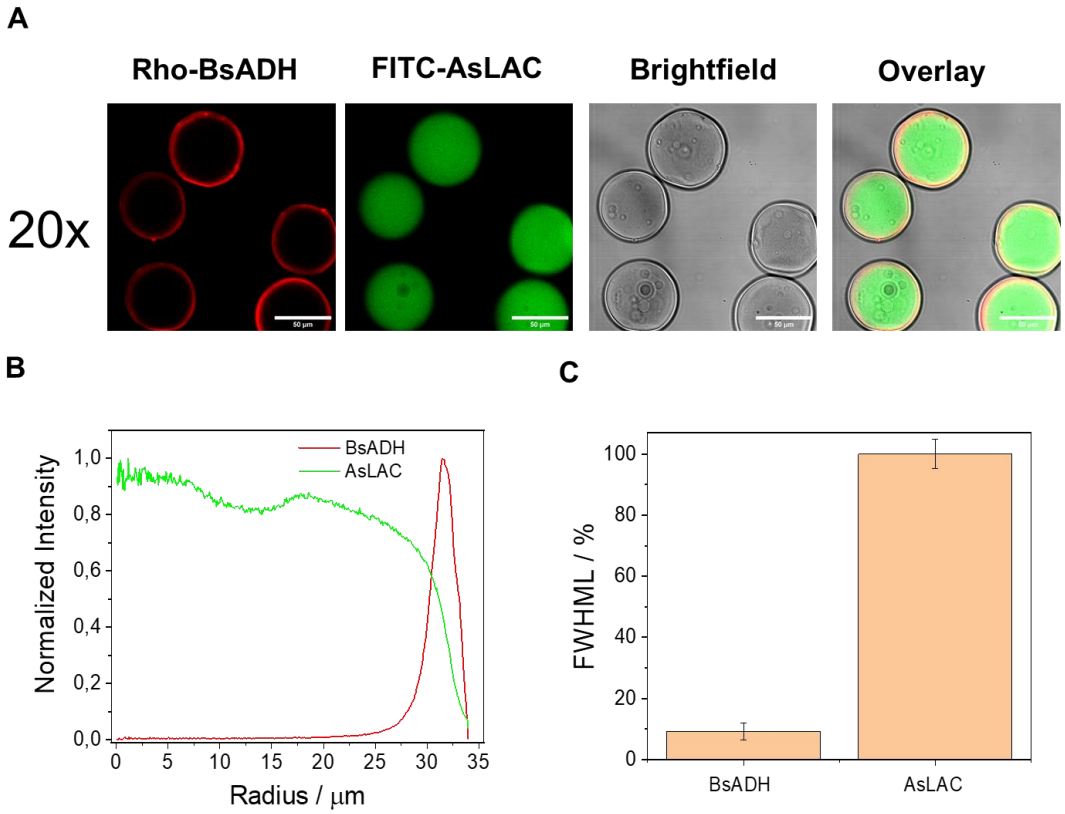

Figure S5. (A) CLSM data showing the spatial distribution of RhoB-BsADH (red) and FITC-AsLAC (green) immobilised in AG-A/Co^{2+} beads. (B) Plot profile showing the distribution of RhoB-BsADH (red) and FITC-AsLAC (green) as relative intensity from the center of AG-A/Co^{2+} beads. (C) Mean of bead radius (FWHML) colonized by either BsADH or AsLAC. Statistical analysis was performed with n =10 microbeads. The values in panel C are the mean value and the standard deviation of that mean value.

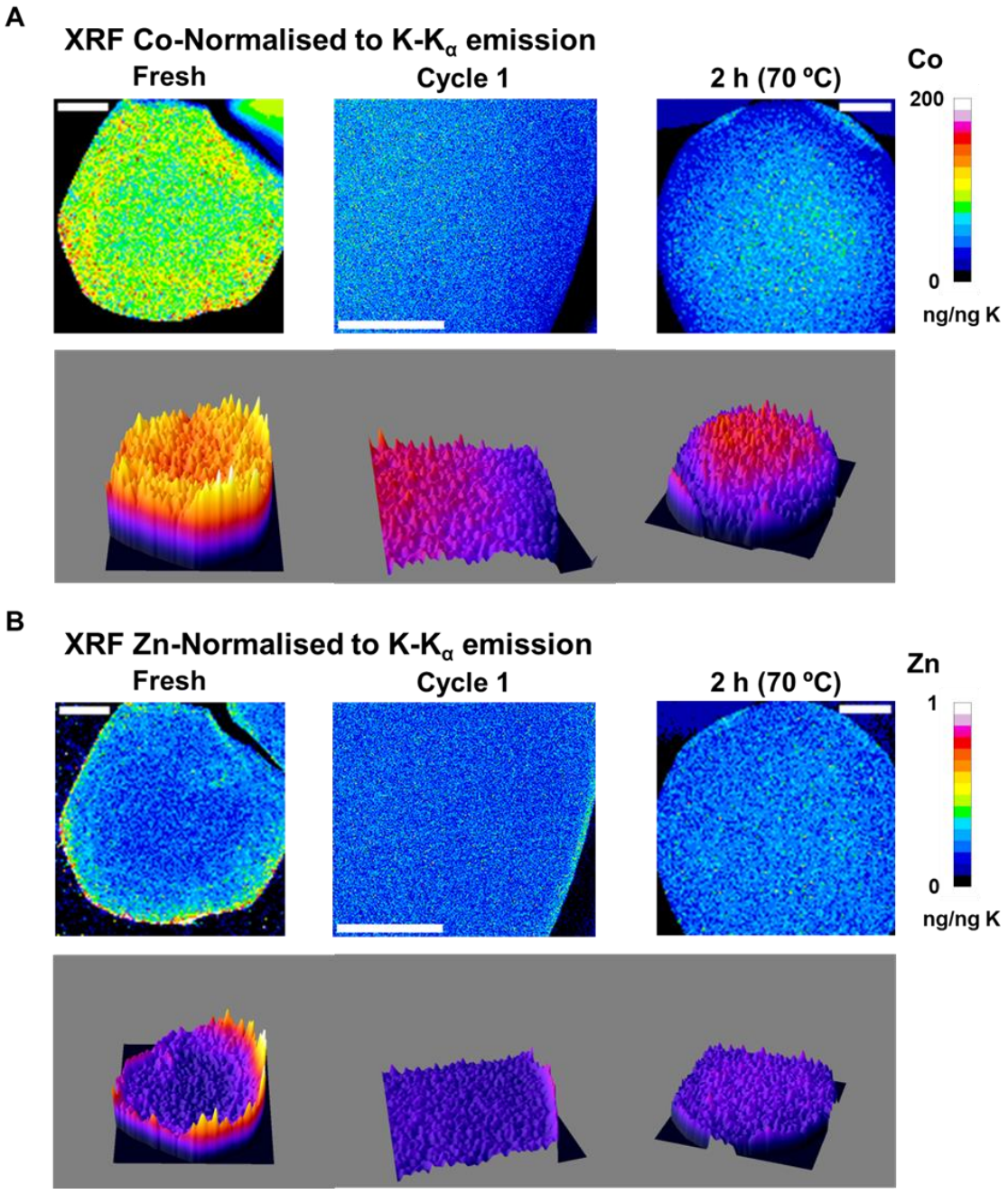

Figure S6. Quantitative XRF maps (top) and 3D intensity profile plots (bottom) of Co (A) and Zn (B) normalised to K content/pixel of fresh (left), 1st reaction cycle (Cycle 1; centre) and thermal inactivated (2h, 70 ºC; right) AG-A/Co^{2+} beads bearing BsADH and AsLAC. Pixel intensity in XRF maps represents metal density according to colour scale. Scale bar 10 µm.

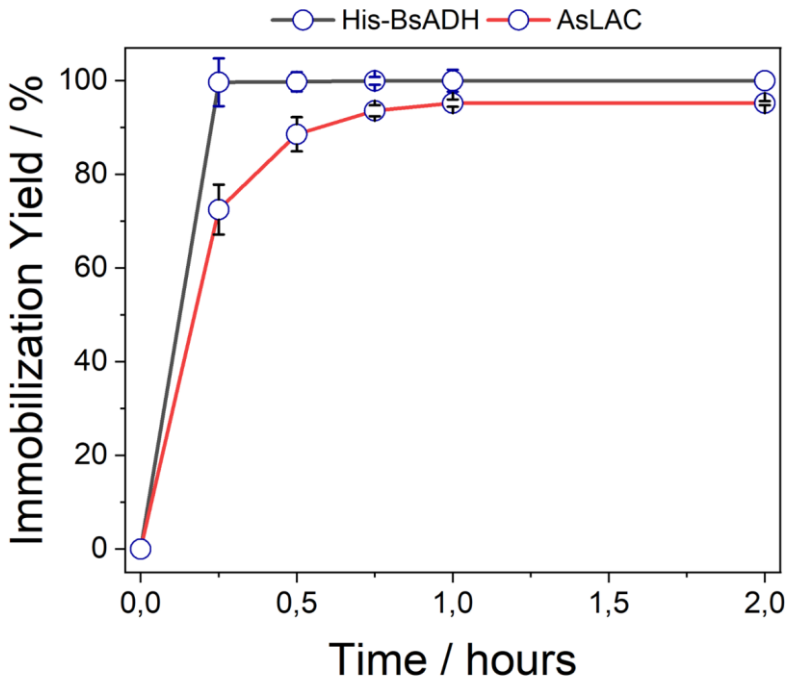

Figure S7. Time dependent immobilisation of AsLAC and BsADH on AG-A or AG-Co^{2+}supports (respectively).

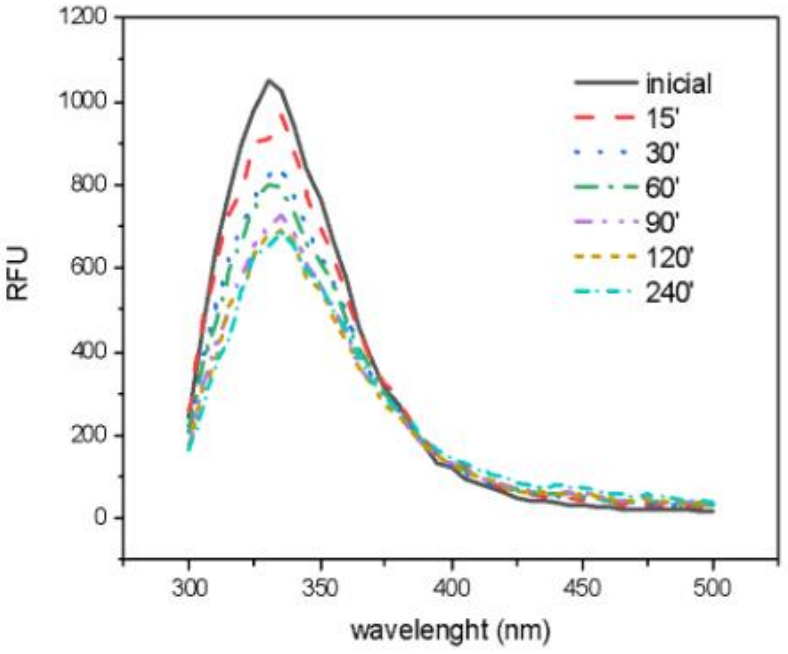

Figure S8. Protein fluorescence spectra from AG-A/Co^{2+} beads bearing BsADH and AsLAC at different inactivation points.

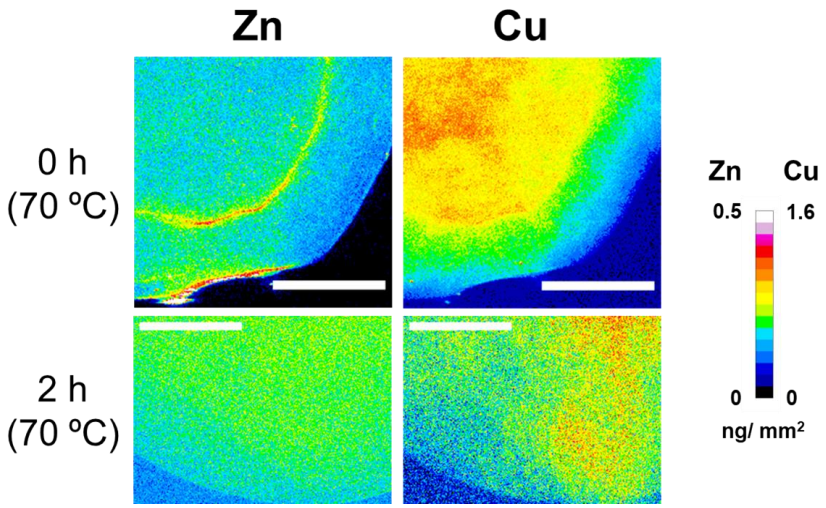

Figure S9. Quantitative XRF maps of Zn and Cu of fresh (0h, 70 ºC; top) and thermal inactivated (2h, 70 ºC; bottom) AG-A/Co^{2+} beads bearing BsADH and AsLAC. Pixel intensity in XRF maps represents metal density according to colour scale. Scale bar 10 µm.

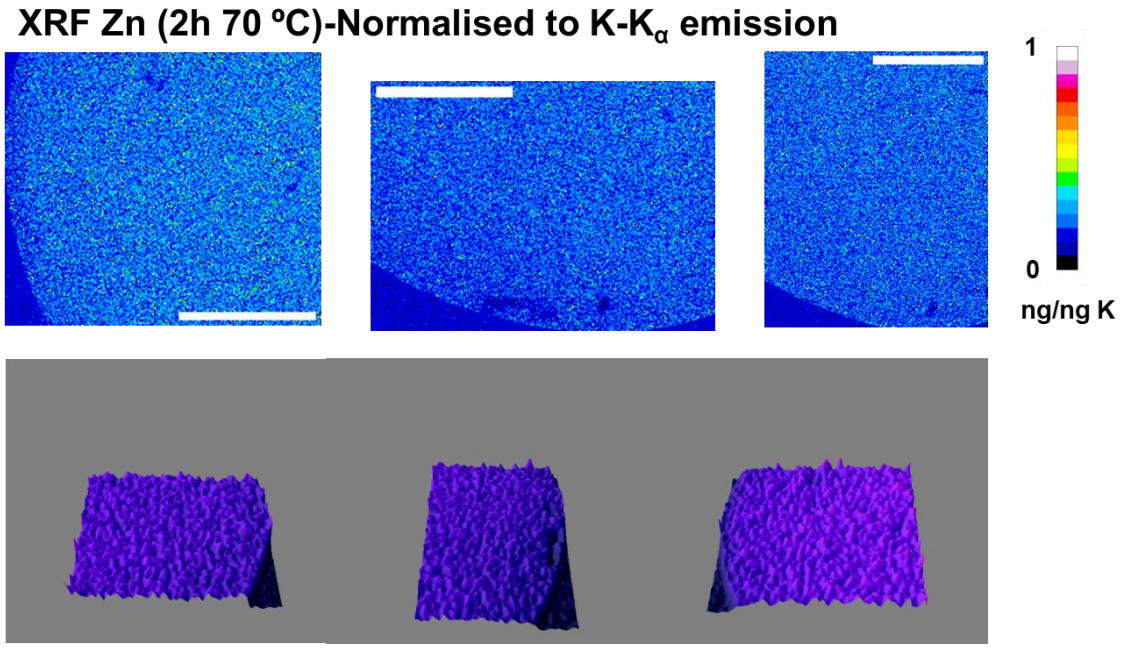

Figure S10. Quantitative XRF maps (top) and 3D intensity profile plots (bottom) of Zn normalised to K content/pixel of several thermal inactivated (2h, 70 ºC) AG-A/Co^{2+} beads bearing BsADH and AsLAC. Pixel intensity in XRF maps represents metal density according to colour scale. Scale bar 10 µm.

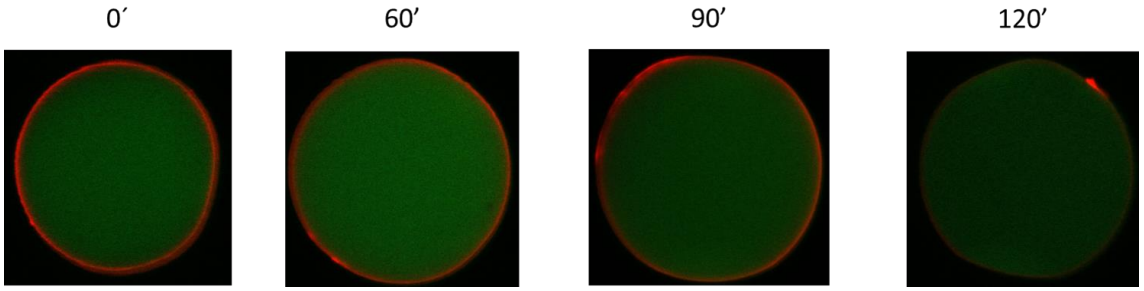

Figure S11. CLSM data showing the spatial distribution of Rho-BsADH (red) and FITC-AsLAC (green) immobilised in AG-A/Co^{2+} beads at different thermal inactivation times at 70 ºC.

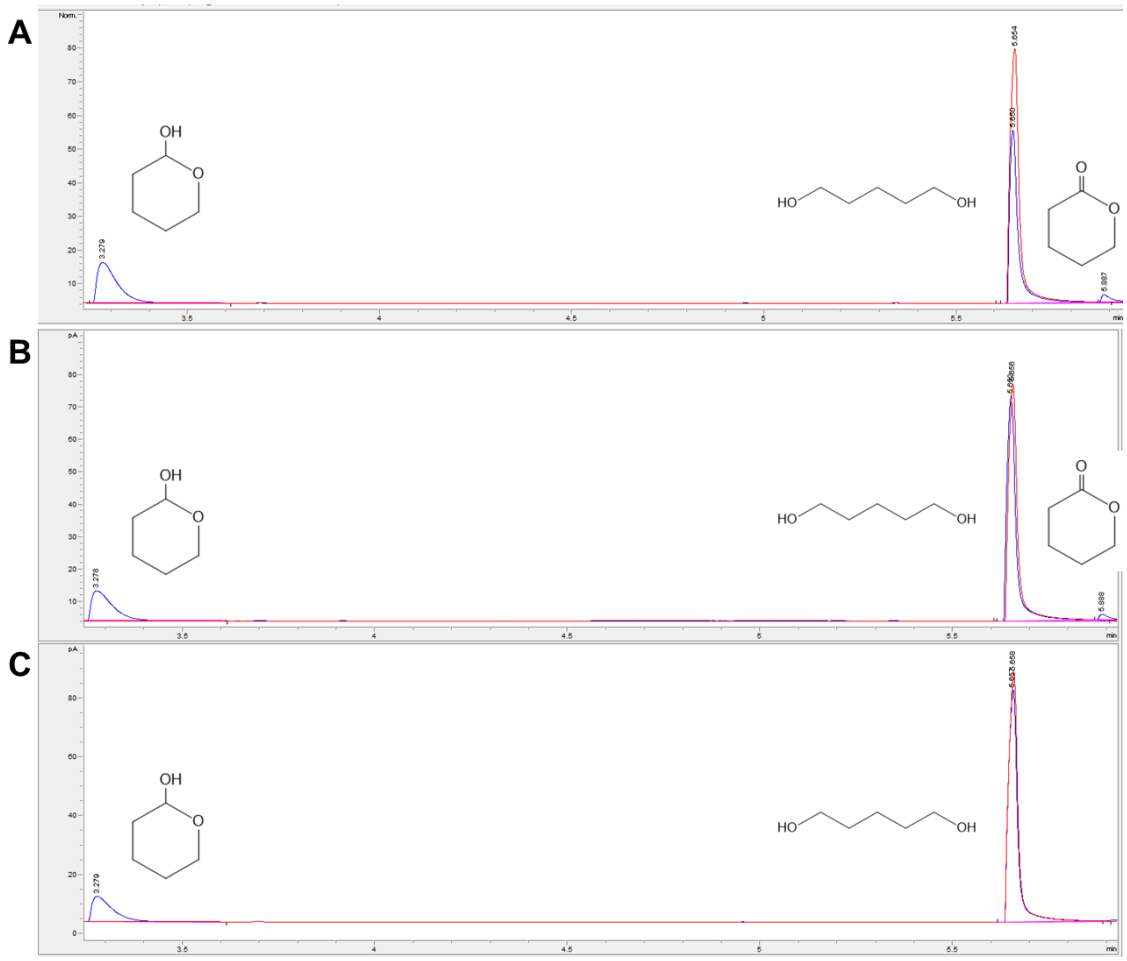

Figure S12. GC-FID chromatogram of the first (A), second (B) and third (C) reaction cycles for the oxidation of 1,5-pentanodiol (20 mM) using AG-A/Co^{2+} beads bearing BsADH and AsLAC (with 1 mM NAD^+, 1 mM acetosyringone at pH 7 and 25º C).

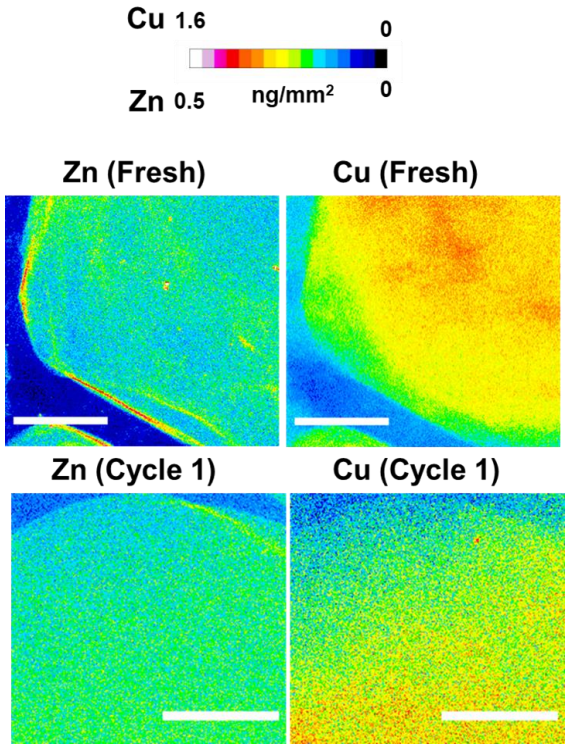

Figure S13. Quantitative XRF maps of Zn and Cu of fresh (0h, 70 ºC; top) and 1st reaction cycle (Cycle 1; bottom) AG-A/Co^{2+} beads bearing BsADH and AsLAC. Pixel intensity in XRF maps represents metal density according to colour scale. Scale bar 10 µm.

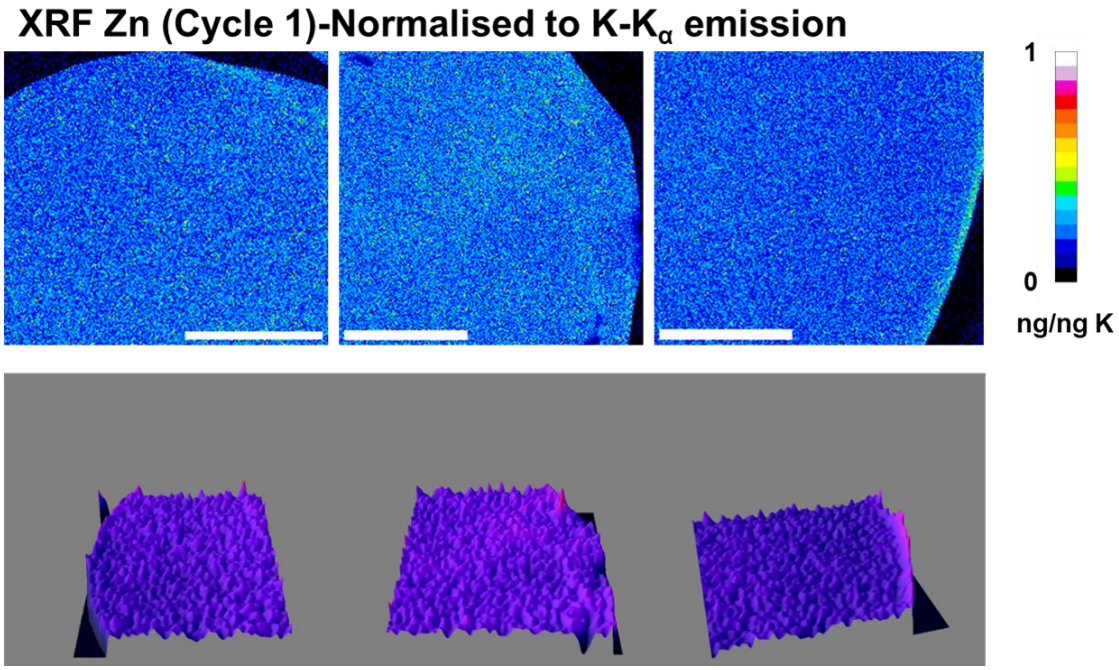

Figure S14. Quantitative XRF maps (top) and 3D intensity profile plots (bottom) of Zn normalised to K content/pixel of several 1st reaction cycle (Cycle 1) AG-A/Co^{2+} beads bearing BsADH and AsLAC. Pixel intensity in XRF maps represents metal density according to colour scale. Scale bar 10 µm.

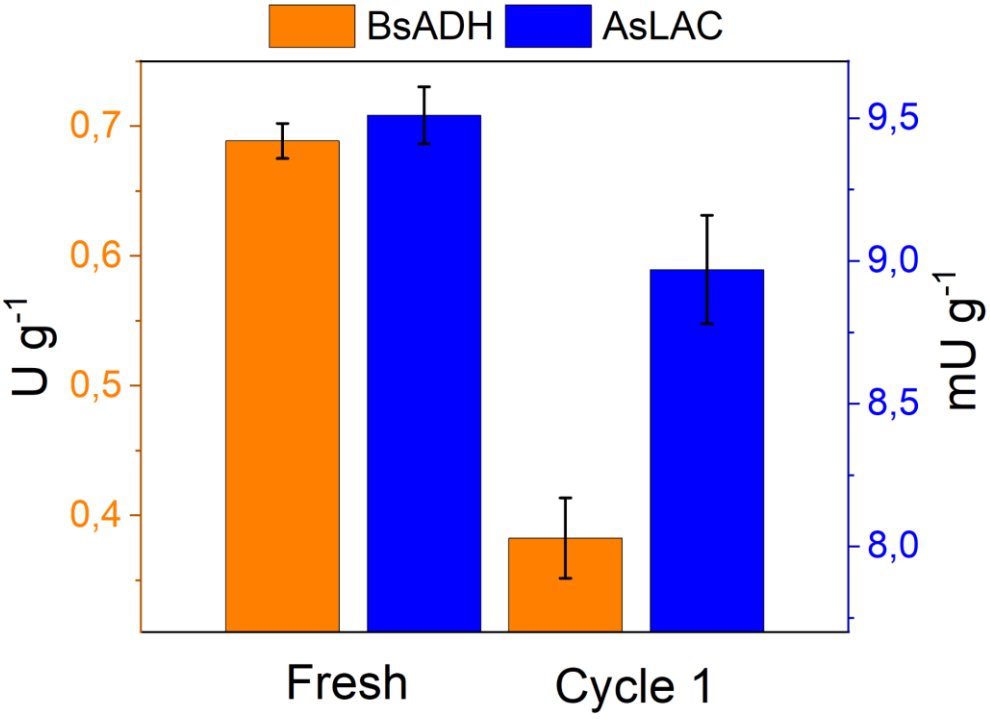

Figure S15. Recovered activity after different reaction cycles using the BsADH and AsLAC co-immobilized on AG-A/Co^{2+} beads. Reaction conditions: 20 mM of 1,5-pentanediol, 1 mM of NAD^+, 1 mM of acetoseryngone in 5 mM sodium phosphate buffer pH 7.

References

1. S. Velasco-Lozano, J. Santiago-Arcos, J. A. Mayoral and F. López-Gallego, *ChemCatChem,* 2020, **12,** 3030-3041.
2. J. Santiago-Arcos, S. Velasco-Lozano and F. López-Gallego, *Biomacromolecules,* 2023, **24,** 929-942.
3. C. Mateo, J. M. Bolivar, C. A. Godoy, J. Rocha-Martin, B. C. Pessela, J. A. Curiel, R. Muñoz, J. M. Guisan and G. Fernández-Lorente, *Biomacromolecules*, 2010, **11**, 3112-3117.
4. J. Santiago-Arcos, S. Velasco-Lozano, E. Diamanti, A. L. Cortajarena, and F. López-Gallego, *Front. Catal.*, 2021, **1**, 715075.
5. K. L. Holmes and L. M. Lantz, *Methods in Cell Biol.*, 2001, **63**, 185-204.
6. J. Schindelin, I. Arganda-Carreras, E. Frise, V. Kaynig, M. Longair, T. Pietzsch, S. Preibisch, C. Rueden, S. Saalfeld, B. Schmid, J.-Y. Tinevez, D. J. White, V. Hartenstein, K. Eliceiri, P. Tomancak and A. Cardona, *Nat. Methods*, 2012, **9**, 676-682.
7. E. Diamanti, S. Arana-Peña, P. Ramos-Cabrer, N. Comino, D. Carballares, R. Fernandez-Lafuente and F. López-Gallego, *Adv. Mater. Interfaces*, 2022, **9**, 2200263.
8. V. A. Solé, E. Papillon, M. Cotte, P. Walter and J. Susini, *Spectrochim. Acta Part B Spectrosc.*, 2007, **62**, 63-68.